Triaxial Compression Results on Core from Borehole U-15n, NNSS, in support of SPE

Scott Broome and Moo Lee
Geomechanics (08864)
Sandia National Laboratories
PO Box 5800, MS 1033
Albuquerque, New Mexico 87185-1033

Abstract

Triaxial compression tests from core hole U-15n are part of a larger material characterization effort for the Source Physics Experiment (SPE) project. This larger effort encompasses characterizing Climax Stock granite rock from the Nevada National Security Site (NNSS) both before and after each SPE shot. The current test series includes triaxial compression tests on dry and saturated intact granite and fault material at 100, 200, 300, and 400 MPa confining pressure.

Background

All triaxial testing reported upon herein came from the U-15n core hole before any SPE shot was conducted; the core hole is drilled in granitic rock (quartz monzonite). U-15n core hole was drilled at the location of the central SPE borehole, and thus closely represents material in which the explosive charges have occurred. There are two fault zones within U-15n (Townsend 2012). Fault #1 and fault #2 intersect U-15n at depths of approximately 82 feet and 107 feet respectively. Specimens for triaxial tests were selected from two distinct depth regions; one of these regions corresponds to fault #1 and the other region is around a depth of 150 feet and is strong intact granite. To date, the U-15n location has been the site of three SPE's (SPE-1, SPE-2, and SPE-3) in Area 15 of the NNSS. The fourth SPE shot is scheduled in the late 2013 timeframe.

Specimen Preparation and Experimental Methods

Specimen Preparation: Test specimens (right circular cylinders) were prepared from the 63.5 mm (2.5 inch) diameter field core by cutting them to approximate length using a standard rock saw, turning the core down to ~50.8 mm (2.0 inches) on a lathe, and then grinding the ends flat and parallel to final length such that the length-to-diameter ratio, L:D, on each test specimen is 2:1. Two types of rock were tested; intact and fault material. Intact specimens were turned down on the lathe dry whereas both the sawing and the grinding used standard tap water for cooling. All preparation steps for fault material specimens were performed dry. Specimens were sized to provide representative results given the maximum grain size of this granite ranges from 0.5-6.35 mm (0.02-0.25 in). Phenocrysts in small quantities were observed along the core length and are as large as ~25.4 mm (1.0 inch) across. The specimen diameter of two inches is slightly less than ten times the maximum observed grain size, however this diameter was necessary in order not to exceed the load frame capacity of 5 MN (1000 kip) during triaxial testing. The dimensions and mass of each specimen were measured to determine specimen density and

porosity. Field cores used in preparing the test specimens were selected from primarily two depths; fault material specimens were near a fault zone at 82 feet depth and intact specimens were from ~150 feet depth. These two distinct depth regions were chosen to represent the end members of the range of strength observed from previous unconfined compression testing. Each piece of field core had a useable length of approximately 127.0-152.4 mm (5.0-6.0 inches) so that the 101.6 mm (4.0 inch) long specimens were prepared with sufficient material available near one end of each core to obtain thin sections and/or thicker billets of untested rock.

Because the natural water table saturates the in-situ rock, TXC tests were conducted on both intact and fault material specimens in dry and saturated conditions. Drying of specimens was conducted in an oven at ~85˚C until no measurable weight loss occurred. Specimens were saturated with tap water in a bell jar using a vacuum until no significant weight gain occurred. Periodically, the bell jar was returned to ambient pressure to allow water to infiltrate the specimen, replacing the air removed from the evacuated specimens. Figure 1 shows typical plots of specimen weight gain versus time. The fault material sample took ~23 days to reach saturation whereas the intact specimen took much longer (~80 days). The intact granite is likely tighter and therefore filling the pore space with water (albeit an order of magnitude less water) takes longer than for the fault material specimens. The data in Figure 1 allows calculation of specimen porosity by imbibition from:

$$\varphi = 100 - \frac{V_I}{V_F} * 100 \tag{1}$$

where φ = % porosity, V_I = initial specimen volume, and V_F = final specimen volume. Final specimen volume is determined from the weight gained from water (i.e. 1 gram of water = 1cc of water).

One sample was tested from a depth of 152.8 feet. The sample had been waxed in the field shortly after the core was retrieved from the coring rig. Effort was made to preserve the as received moisture content of the waxed sample.

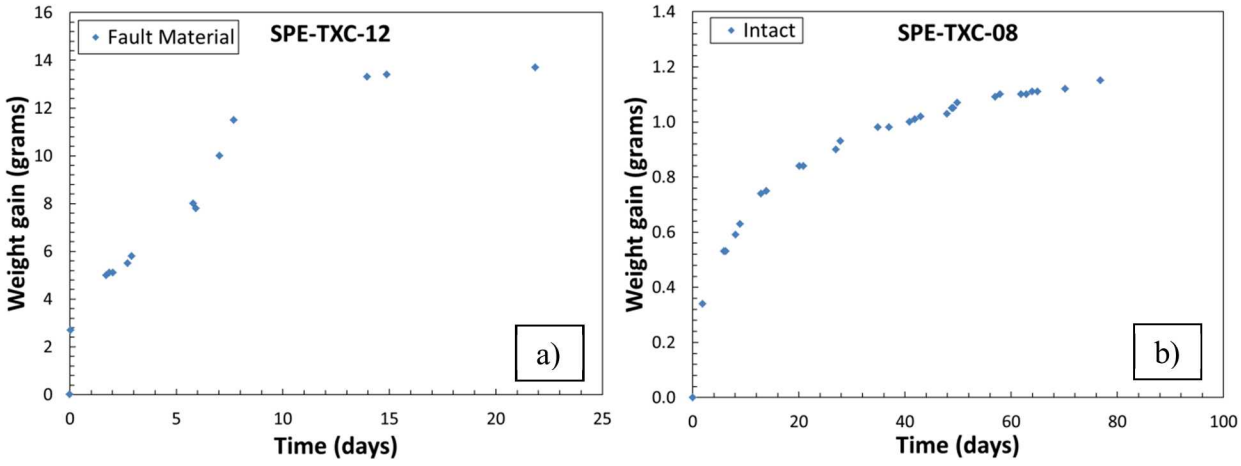

Figure 1: Weight gain of water versus time for a) fault material specimen and b) intact specimen.

Bulk Density Determination: The bulk density of each TXC test specimen was determined from its mass and volume; volume is calculated using dimensional measurements assuming a right-circular-cylindrical geometry. Density was determined on saturated samples in the saturated state.

Triaxial Compressive Strength (TXC) Testing: Tests were run on both fault material and fresh granite both in dry and saturated states to determine if there are differences in mechanical properties over these four conditions. All tests were performed undrained. However during the application of confining pressure for fault material tests, pore pressure was vented such that at the start of application of differential stress, the pore pressure was a very low percentage of the confining pressure. Venting of pore pressure of the aforementioned specimens was necessary for two reasons: 1) to avoid a low and undetermined effective confining pressure test (i.e. pore pressure had increased to the same level as confining pressure) and 2) to ensure that a jacket leak had not occurred during pressurization (if pore pressure is vented and there is a jacket leak, confining fluid will most likely release from the pore vent). All specimens were instrumented to measure axial force (from which axial stress was calculated), confining pressure, and pore pressure (for saturated specimens). Axial and radial strains were calculated from LVDT's mounted on specimen end-caps and directly near mid-height on the specimen respectively.

Confining pressure was applied at a constant rate of 0.05 MPa/sec. Unload/reload loops were performed at various confining pressures to estimate Bulk modulus, K as a function of confining pressure. Specimens were then loaded quasi-statically in compression (axial strain rate of $\sim 1^{x}10^{-4}$/sec) under constant confining pressure and ambient temperature conditions. Loading continued until the peak axial stress was observed. All samples were loaded to failure and if possible, post failure behavior was captured. During loading and if possible post failure, unload/reload cycles were performed at various axial stress levels to acquire data to estimate the compressive elastic properties – Young's modulus, E_c, and Poisson's ratio, v_c. Figure 2 shows an instrumented specimen mounted on the base of the 400 MPa capacity pressure vessel used for all TXC tests.

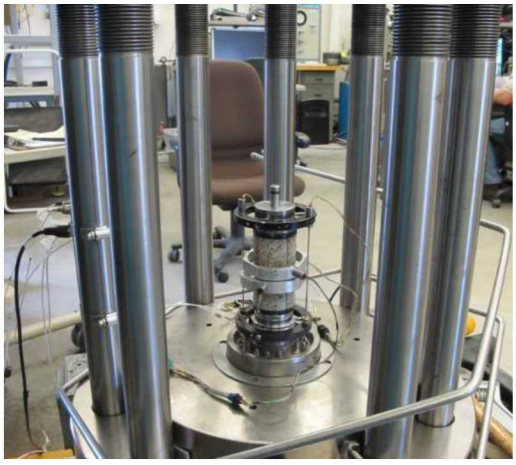

Figure 2: Specimen mounted on the base of the 400 MPa pressure vessel used for all TXC tests.

Compressional and Shear Wave Velocity Measurements: Ultrasonic compressional and shear wave velocity measurements, V_p and V_s, were performed on each TXC specimen under ambient conditions prior to TXC testing. Wave speed measurements were made coincident with each specimen axis and also orthogonal to the axis across two diameters separated by 90^0. Velocity measurements for saturated samples were made after specimen saturation and in some cases prior to saturation.

Experimental Results

Table 1 lists the depth, dimensions, weight, density, and test date for each TXC test. All specimens were taken from borehole U-15n before any SPE event. Tests highlighted in red in the comments column indicate samples that suffered from jacket leaks. Other tests in the comments column are highlighted to indicate one of five test material/test conditions as follows:

1) Fault Material/Dry (F/D)
2) Fault Material/Saturated (F/S)
3) Intact/Dry (I/D)
4) Intact/Saturated (I/S)
5) Intact/Wax (I/W)

All TXC bulk modulus (K) data is combined in Figure 3 and is plotted against confining pressure. Figure 3 shows that saturated fault material has the lowest K values. Dry fault material and intact wet/wax granite has intermediate K values and intact dry granite has the highest values of K. Note that K values (32, 41, 49 and 51GPa) for the intact waxed specimen (SPE-TXC-11) fall within the scatter of the intact saturated tests and that the density of SPE-TXC-11 (2.66 g/cc) is the average density of the intact saturated samples. This data indicate that the in-situ intact granite at a depth of ~150 feet is in a saturated state (i.e. likely below the water table).

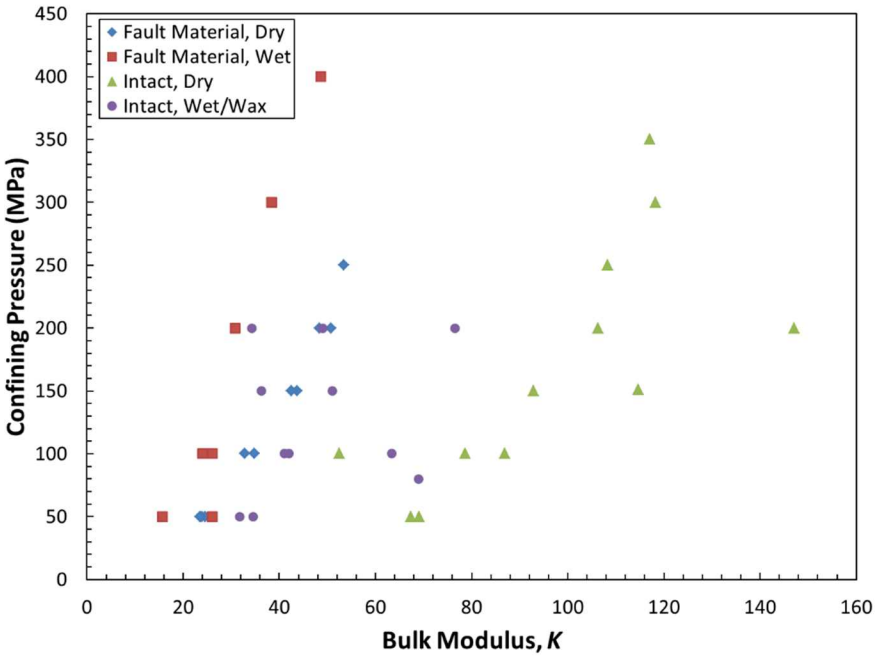

Figure 3: Confining pressure versus bulk modulus for all triaxial tests.

Table 2 lists sample porosity determined by equation (1) for all specimens saturated with tap water. Fault material specimens have on average one order of magnitude greater porosity than intact granite specimens.

Table 1. Sample #, Depth, Diameter, Length, Weight, Density, Test Date, Comments

Sample	Depth (ft)	Diameter (cm)	Length (cm)	Weight (g)	Density (g/cc)	Test Date	Comments
SPE-TXC-01	75	5.072	10.465	542.0	2.56	2/28/2012	Fault Material-Dry-σ_C=200
SPE-TXC-02	84	5.075	10.881	563.6	2.56	2/29/2012	Fault Material-Dry-σ_C=400
SPE-TXC-03	85	5.075	10.688	553.1	2.56	3/14/2012	Fault Material-Wet-σ_C=200
SPE-TXC-04	87	5.080	10.930	564.7	2.55	3/26/2012	Fault Material-Wet-Leak-σ_C=100
SPE-TXC-05	153.4	5.090	10.587	569.3	2.64	4/3/2012	Fresh-Dry-σ_C=200
SPE-TXC-06	152.1	5.080	10.833	583.5	2.66	4/11/2012	Fresh-Dry-Leak-σ_C=300
SPE-TXC-07	151.2	5.083	10.734	581.2	2.67	6/13/2012	Fresh-Wet-σ_C=200
SPE-TXC-08	147.7	5.093	10.770	581.1	2.65	6/26/2012	Fresh-Wet-σ_C=400
SPE-TXC-09	150.1	5.083	10.886	582.9	2.64	4/18/2012	Fresh-Dry-Leak-σ_C=400
SPE-TXC-10	75.8R	5.088	10.759	556.75	2.55	6/12/2012	Fault Material-Wet-σ_C=100
SPE-TXC-11	152.8	5.098	10.739	582.08	2.66	11/9/2012	Fresh-Waxed-σ_C=200
SPE-TXC-12	75.8L	5.075	10.775	559.21	2.57	10/31/2012	Fault Material-Wet-σ_C=400
SPE-TXC-13	178	5.080	10.701	577.90	2.66	5/15/2012	Fresh-Dry-Leak-σ_C=400
SPE-TXC-14	140.6	5.075	10.757	576.10	2.65	7/11/2012	Fresh-Dry-σ_C=400

Table 2. Sample #, Porosity (%), Rock Type

Sample	φ (%)	Rock Type
SPE-TXC-03	9.77	Fault Material
SPE-TXC-04	9.15	Fault Material
SPE-TXC-07	0.73	Intact Granite
SPE-TXC-08	0.52	Intact Granite
SPE-TXC-10	8.26	Fault Material
SPE-TXC-12	5.91	Fault Material

Table 3 shows how Young's modulus, E and Poisson's ratio, v for TXC tests vary as differential stress is increased. In general, E compares closely with unconfined results from U-15n and U-15n#10 (Broome and Pfeifle (2011) and Broome and Lee (2012)); the intact granite is ~80 GPa and fault material is ~50 GPa. It should be noted that a change in nomenclature has transpired; fault material in previous reports was called weathered granite. Failure stress, shown in the far right column in Table 3, increases as confining pressure increases with the exception for saturated fault material. Effective confining stress is determined as follows:

$$\sigma_{2,3(effective)} = \sigma_C - \sigma_P \tag{2}$$

where σ_C is confining pressure and σ_P is pore pressure.

There is a wide variance between the strength of saturated fault material compared to dry fault material. Intact material strength varies little between dry, waxed and saturated moisture states. Lateral LVDT's failed electrically for test SPE-TXC-14 and therefore v was not determined (entries are designated at N/A).

Table 3: Test #, Depth, Material/Condition, Young's modulus (E), Poisson's ratio (v), Effective confining pressure ($\sigma_{2,3\ (effective)}$), Differential stress at calculated E and v (σ_D), and Differential stress at failure ($\sigma_{D,F}$).

Test	Depth (ft)	Material/ Condition*	E (GPa)	v	$\sigma_{2,3\ (effective)}$ (MPa)	σ_D (MPa)	$\sigma_{D,F}$ (MPa)
SPE-TXC-01	75	F/D	49.6	0.24	200	80	379
SPE-TCX-01	75	F/D	48.1	0.25	200	175	379
SPE-TXC-02	84	F/D	55.3	0.03	400	90	816
SPE-TXC-02	84	F/D	26.7	0.12	400	285	816
SPE-TXC-02	84	F/D	26.8	0.12	400	455	816
SPE-TXC-10	76	F/S	17.8	0.53	1	32	88
SPE-TXC-10	76	F/S	19.1	0.48	7	63	88
SPE-TXC-10	76	F/S	18.6**	0.44**	15	88	88
SPE-TXC-10	76	F/S	18.2**	0.50**	25	73	88
SPE-TXC-03	85	F/S	13.2	0.52	195	32	50
SPE-TXC-03	85	F/S	6.5**	0.56**	192	18	50
SPE-TXC-03	85	F/S	6.4**	0.62**	192	17	50
SPE-TXC-12	76	F/S	82.2	0.10	400	56	174
SPE-TXC-12	76	F/S	53.2	0.30	400	91	174
SPE-TXC-12	76	F/S	49.4	0.29	400	134	174
SPE-TXC-12	76	F/S	72.5	0.07	400	174	174
SPE-TXC-05	153	I/D	85.5	0.12	200	86	990
SPE-TXC-05	153	I/D	76.7	0.15	200	188	990
SPE-TXC-05	153	I/D	75.4	0.16	200	319	990

Test	Depth (ft)	Material / Condition*	*E (GPa)*	*v*	$\sigma_{2,3\ (effective)}$ *(MPa)*	σ_D *(MPa)*	$\sigma_{D,F}$ *(MPa)*
SPE-TXC-05	153	I/D	75.6	0.18	200	477	990
SPE-TXC-05	153	I/D	72.2	0.20	200	667	990
SPE-TXC-06	152	I/D	83.0	0.20	300	153	1115
SPE-TXC-06	152	I/D	72.7	0.20	300	424	1115
SPE-TXC-06	152	I/D	70.0	0.22	300	825	1115
SPE-TXC-06	152	I/D	72.3	0.25	300	1055	1115
SPE-TXC-14	141	I/D	72.9	N/A	400	108	1265
SPE-TXC-14	141	I/D	67.9	N/A	400	377	1265
SPE-TXC-14	141	I/D	70.3	N/A	400	715	1265
SPE-TXC-07	151	I/S	67.9	0.22	200	92	902
SPE-TXC-07	151	I/S	64.5	0.22	200	221	902
SPE-TXC-07	151	I/S	64.2	0.25	200	592	902
SPE-TXC-08	148	I/S	93.4	0.19	400	146	1246
SPE-TXC-08	148	I/S	86.1	0.21	400	435	1246
SPE-TXC-08	148	I/S	82.7	0.23	400	655	1246
SPE-TXC-11	153	I/W	71.4	0.09	200	60	952
SPE-TXC-11	153	I/W	72.1	0.13	200	101	952
SPE-TXC-11	153	I/W	69.3	0.16	200	144	952
SPE-TXC-11	153	I/W	75.2	0.13	200	189	952
SPE-TXC-11	153	I/W	72.2	0.16	200	276	952
SPE-TXC-11	153	I/W	68.6	0.20	200	395	952
SPE-TXC-11	153	I/W	68.9	0.21	200	503	952
SPE-TXC-11	153	I/W	68.9	0.21	200	611	952

*First letter: F = Fault Material, I = Intact granite
*Second letter: S = Saturated, D = Dry, W = Wax
**Elastic properties obtained post failure
Properties in red obtained using load frame displacement transducer

Plots of confining pressure versus true strain and true differential stress versus true strain for all eleven TXC tests are presented in report SAND2013-2913P. Volumetric strain is calculated from the measured axial and radial strains, i.e., $\varepsilon_v = \varepsilon_{ax} + 2\varepsilon_{rad}$.

Table 4 lists the results from ultrasonic compressional and shear wave velocity measurements taken coincident with each specimen axis. Velocity measurements taken orthogonal to the axis across two diameters separated by 90° respectively are listed in tables in report SAND2013-2913P.

Dynamic Young's modulus ranges from approximately 43.5 to 101.2 GPa and dynamic Poisson's ratio ranges from approximately 0.09 to 0.31 for all samples measured in the axial direction.

Table 4. P- and S-wave travel time and velocity and calculated values of dynamic *E* and *v* along core axis.

	Axial					
Sample #	P Wave Travel Time (µs)	P-Velocity (km/s)	S Wave Travel Time (µs)	S-Velocity (km/s)	$E_{Dynamic}$ (GPa)	$v_{Dynamic}$
SPE-TXC-01	21.57	4.9131	41.02	2.5680	44.35	0.31
SPE-TXC-02	23.08	4.7704	38.63	2.8366	50.54	0.23
SPE-TXC-03	23.14	4.6735	41.78	2.5749	43.49	0.28
SPE-TXC-04	23.65	4.6748	40.48	2.7181	46.88	0.24
SPE-TXC-05	17.97	5.9812	30.48	3.5044	80.39	0.24
SPE-TXC-06	17.68	6.2223	26.15	4.1859	101.20	0.09
SPE-TXC-07	18.25	5.9700	31.15	3.4760	80.20	0.24
SPE-TXC-07 (wet)	18.35	5.9370	31.28	3.4615	79.46	0.24
SPE-TXC-08 (wet)	18.28	5.9798	30.78	3.5299	81.36	0.23
SPE-TXC-09	18.56	5.9521	31.86	3.4462	78.23	0.25
SPE-TXC-10	22.18	4.9107	38.07	2.8464	51.43	0.25
SPE-TXC-11 (wax)	17.80	6.1261	31.72	3.4147	78.94	0.27
SPE-TXC-12	22.28	4.8954	36.57	2.9682	54.67	0.21
SPE-TXC-13	17.98	6.0424	30.37	3.5552	83.20	0.24
SPE-TXC-14	18.56	5.8813	31.44	3.4510	78.04	0.24

Analysis of Results

All triaxial data (acquired at an axial strain rate of 10^{-4} s^{-1}) are presented in Figure 4 in true differential stress versus true mean normal stress space. A stress path for each test is plotted leading up to the failure or maximum differential stress point denoted by either a triangle or dot. Black data points represent failure for dry tests and blue data points represent failure for saturated or waxed tests.

Two trend lines with their equations are shown in Figure 4. The curved trend line represents a best fit through dry intact material failure points. The flatter trend line represents a best fit through dry fault material failure points. At this range of confining pressures, the opposite trend was expected from that shown in Figure 4; failure points for fault material were expected to produce more of a curve fit than failure points for intact material because the fault material was expected to reach a "knee" on the failure surface before the intact material. Lack of test

repeatability means the single dry fault material test at 400 MPa confining pressure could be statistically high and is pulling the curve fit up. The saturated and waxed intact tests are lower but also very close in strength to dry intact tests; this is not the case with fault material where saturated tests are much weaker than their dry counterparts.

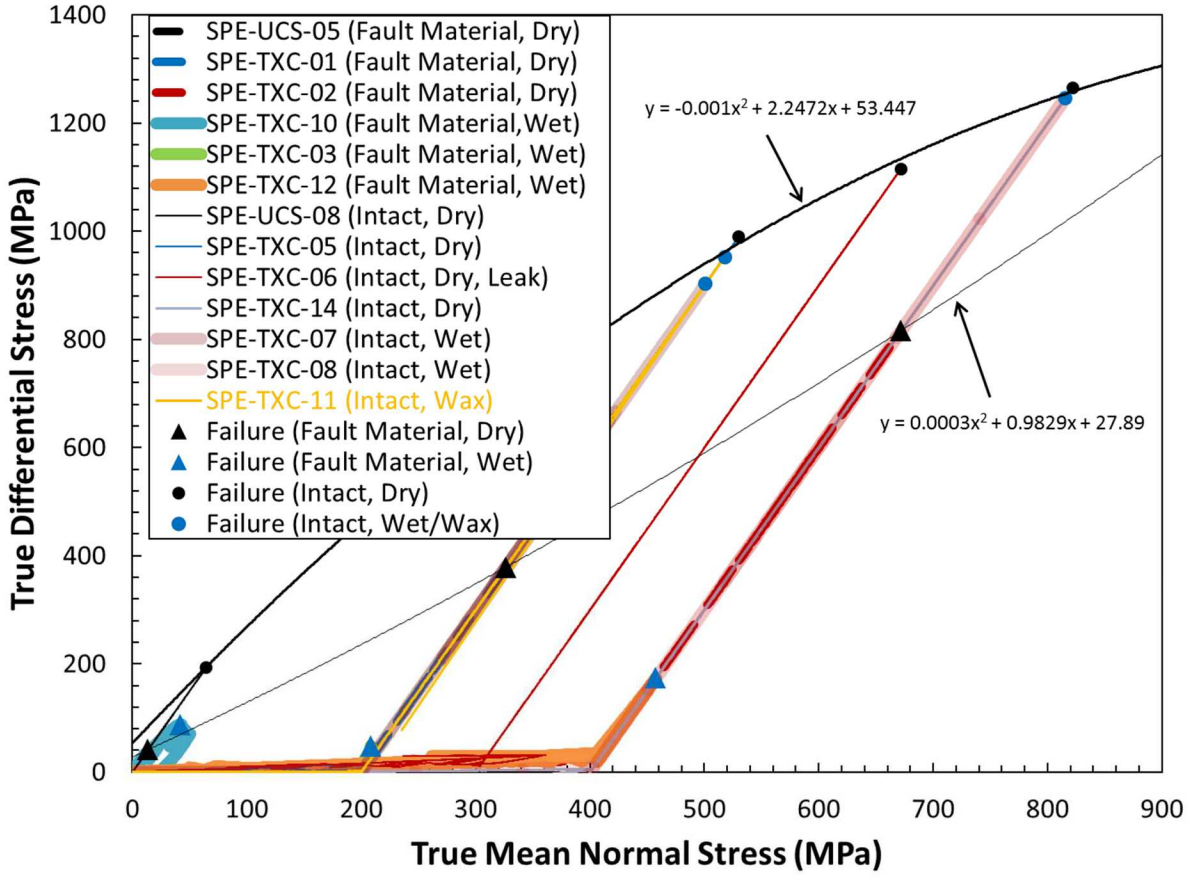

Figure 4: Stress paths and failure stress for all undrained TXC tests conducted at an axial strain rate of 10^{-4} s^{-1}.

As discussed above, Young's modulus was determined using two methods: 1) directly from stress-displacement data acquired during quasi-static unload/reload cycles and 2) indirectly calculated from density and compressional and shear wave velocity measurements. Quasi-static Young's modulus can be analyzed in five distinct groups:

- Fault Material, Dry (Tests 1 and 2)
- Fault Material, Wet (Tests 3, 10, and 12)
- Intact Granite, Dry (Tests 5, 6, and 14)
- Intact Granite, Wet (Tests 7 and 8)
- Intact Granite, Wax (Test 11)

From Tables 3 and 4, both quasi-static and dynamic Young's modulus values for fault material are lower than values for intact granite. Saturation of fault material has a greater effect on

Young's modulus values than saturation of intact granite; the same trend is evident for failure stress shown in Figure 4.

From Tables 3 and 4, there was no observable difference in the average Poisson's ratio using either quasi-static or dynamic methods. However, the coefficient of variation (CV) was higher (0.57) for quasi-static tests than Poisson's ratio determined dynamically (CV = 0.20). The primary reason for the difference in CV is that wet fault material specimens gave higher Poisson ratios than dry fault material specimens; dynamic Poisson's ratio was not determined for saturated fault material specimens. In addition, one sample was measured using the external load frame axial LVDT and Poisson ratio values were low (0.09). In general, the values of Poisson's ratio (both measured quasi-statically and dynamically) ranged from about 0.09 to 0.31.

Conclusions

Fourteen triaxial compression tests from core hole U-15n (the source hole for all SPE shots) have been presented and discussed. All tests were from pre shot core with two material types and two moisture conditions tested; intact granite and fault material both dry and saturated. One intact granite sample was preserved in wax; its density and failure stress indicate its moisture content was likely close to saturated intact granite.

Triaxial compression tests from core hole U-15n are part of a larger material characterization effort for the Source Physics Experiment (SPE) project. This larger effort encompasses characterizing Climax Stock granite rock from the Nevada National Security Site (NNSS) both before and after each SPE shot.

Contents of this report taken from Broome (2013). Broome (2013) contains additional figures, tables, additional discussion of results, and appendices with details of individual tests.

References

Townsend, M., et al., 2012. Projected Extent of Two Faults Encountered in Core Hole U-15n, NSTec UGTA/Boreholes Geology Group, 08 March 2011.

Broome, S. and Pfeifle, T., 2011. Phase 1 Mechanical Property Test Results for Borehole U-15n in Support of NCNS Source Physics Experiment, SAND2011-4394C.

Broome, S. and Lee, M., 2012. Unconfined Compression Mechanical Testing Results on Core from Borehole U-15n#10, Nevada National Security Site, in support of NCNS Source Physics Experiment, SAND2012-9376P.

Broome, S. and Lee, M., 2013. Triaxial compression testing results on core from borehole U-15n, Nevada National Security Site, in support of NCNS Source Physics Experiment, SAND2013-2913P.

Sandia National Laboratories is a multimission laboratory managed and operated by National Technology and Engineering Solutions of Sandia, LLC, a wholly owned

subsidiary of Honeywell International, Inc., for the U.S. Department of Energy's National Nuclear Security Administration under contract DE-NA0003525.